

AUTOMATIC COUNTING METHOD OF TOUCHING WHEAT GRAINS WITH FOURIER ANALYSIS AND SHAPE SIMILARITY METHOD

CHUN YING WANG^{1,2}, MENG LI SUN^{1,2},
LI PENG LIU^{1,2}, PING LIU^{1,2,*}, XIANG LI^{3,4}

¹College of Mechanical and Electronic Engineering,
Shandong Agricultural University, Taian, 271018, China
²Shandong Agricultural Equipment Intelligence Engineering
Laboratory, Taian, 271018, China

³College of Life Sciences, Shandong Agricultural University, Taian, 271018, China

⁴State Key Laboratory of Crop Biology, Taian, 271018, China

*Corresponding Author: liupingsdau@126.com

Abstract

Grain number counting generally relied on image processing which took a long time to detect the corner points of touching grains. This paper aimed to propose a novel method to count touching wheat grains based on Fourier analysis and shape similarity method automatically and rapidly. Firstly, the area threshold method was used to detect the touching wheat grains after image preprocessing. Then, the normalized elliptic Fourier descriptors was used to obtain the shape of touching grains. After that, the grain number of the connected region was identified by shape similarity method using the normalized Fourier descriptors. Finally, the proposed method was tested on wheat grains under different touching scenarios and compared with existing counting methods. The average accuracy of the proposed method was 99.12%. The maximum error rate and the average running time of counting grain number per spike were 2.75% and 1.662 seconds, respectively. What's more, the running time increased with the number of connected regions but was irrelevant to the grain number per connected region. It can eliminate the traditional limitations of low accuracy and high counting time and lay a solid foundation for future estimation of wheat yield.

Keywords: Fourier analysis, Grain counting, Shape similarity method, Touching wheat grains.

1. Introduction

Wheat is one of the most widely grown grains. As a required component of global food security, it provides 20 percent of the total heat needed by the world's growing population [1, 2]. In 2020, the annual global output of wheat was 773.7 million tons. Grain yield is the key indicator for selecting breeding materials [3]. Grain yield is determined by three main factors, including number of spikes per square meter, number of grains per spike, and grain weight. And thousand kernel weight (TKW) was used as an indicator of grain weight [4]. Until recently, the counting of TKW and number of grains per spike was done by image segmentation [5]. The automatic accurate counting grain number can be achieved by the capacity to segment and count of touching wheat kernels. Therefore, efficient, reliable, and automatic counting methods for the wheat grain were required.

For TKM and grain number per spike measurement, counting is important. The wheat grains separated from the image background were marked so that the number of kernels was calculated. The difficulty of counting the grains accurately has been increased by the touching grains. To address this problem, different approaches to separate touching grains have been proposed in the literature, such as the morphological dilation and erosion method [6], the watershed algorithm [4, 7, 8], the feature detection method [9-12], and the neural network [12-14].

The morphological method was a simple and time-saving algorithm, but the human experience was always an important factor in the frequency of erosion and dilation. Some morphological information may be lost after morphological operations. The watershed algorithm was a segmentation method which was used widely [8]. It started from kernel areas under pixel gradient limitations and used local gradient difference in contacting areas to identify division lines through a simulated method of water flooding. The conventional watershed algorithm's fundamental flaw was over separation [15]. In order to reduce over-separation, many recent researches had improved the watershed algorithm. For example, the watershed algorithm controlled by marker combined with the area threshold method was proposed to avoid over-segmentation [4]. Feature detection including curvature detection and corner detection was highly affected by noise and boundary roughness [9, 10, 16]. In order to solve these issues, concave spots were recognized by variations in the response value of a circular template as it moved along the boundary [9, 12]. But in the separation process, the hardest step was concave point pair matching [17, 18], multiple criteria were used to determine splitting lines, including the nearest neighbor criterion and the radian critical distance criterion [10, 19, 20]. To solve the problems of the watershed algorithm and corner point algorithm, Tan et al. [12] proposed an improved algorithm which combined with the watershed algorithm. It was an adaptive-radius circular template-based corner point algorithm and neural network. The average accuracy of this research was 94.63%. To enumerate the number of grains that contacted each other, the watershed algorithm controlled by marker and the area threshold method were proposed [4]. However, there is still great potential for majorization in the efficiency and accuracy of grain counting.

To sum up, the counting of touching grains has used different techniques. Among them, yet they have limitations in several aspects, which take a long time to detect the corner points of touching grains. To reduce the computational effort with acceptable accuracy, a novel method for counting touching wheat grains was

given in this paper, which has the advantages of high accuracy and less counting time. Firstly, elliptic Fourier descriptors was used to capture the shape of the grains [21-25]. Fourier descriptor was considered to be a promising approach for shape description because of the solid theoretical basis [26]. In addition, it had the advantage of attractive invariance properties and high calculation efficiency. The determination of corner locations was carried out after the Fourier analysis in previous research, which increased the computational complexity [10]. Furthermore, to reduce the computational complexity, the relationship between the Fourier descriptors and the grain number of the connected region was identified using the shape similarity method. The regions of touching grains were classified into ten categories: two grains, three grains, four grains, ..., ten grains. Finally, the average accuracy of the proposed method was appraised by the comparison with manual evaluations. Our goal is to give a method for counting touching grains automatically and rapidly, which will provide a reference for investigating the relationships between spike traits, grain number and yield potential, variety breeding, and cultivation management.

2. Material and Methods

2.1. Materials preparation

The experiment was conducted at the experimental station of Shandong Agricultural University, Taian, China. As a selection benchmark, morphological features (such as grain length, width, perimeter, and size) were considered. And three types of wheat were respectively selected. They were Shannong23, Shannong28, and Shannong32. Each plot was 3m long \times 1.2m wide and consisted of 4 rows with a 0.3m inter-row spacing. A sample of forty ears was collected randomly from each plot at physiological maturity on 14 June 2019 and dried to approximately 14% kernel moisture content. These wheat grains were separated manually before being set on our platform to establish the dataset.

2.2. System design

The digital photographs acquisition system used for acquiring images of wheat grains included the mobile phone, background, and frame. The resolution of the phone is 3968 \times 2976 pixels. The background was a blackboard or white luminous board. The grains per spike were placed on the background under the fixed height camera as described in Fig. 1. The distance between the mobile phone and the grains was 20 to 40 cm. A maximum contrast between the grains and the image background was generated to ensure that touching grains could be removed.

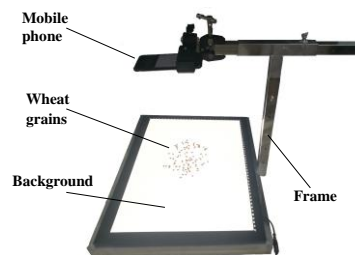


Fig. 1. Digital photographs acquisition system.

2.3. Automatic counting method

This paper aimed to propose a novel method for counting touching wheat grains automatically and rapidly. The workflow diagram overview of the automatic counting method was shown in Fig. 2. The area threshold method was used to detect the touching wheat grains after image preprocessing. Fourier analysis was used to obtain the shape of touching grains. Then, the grain number of the connected region formed by touching grains was identified by shape similarity method using the normalized Fourier descriptors. Finally, the grain number in the connected region was counted, and the grain number per spike was further obtained.

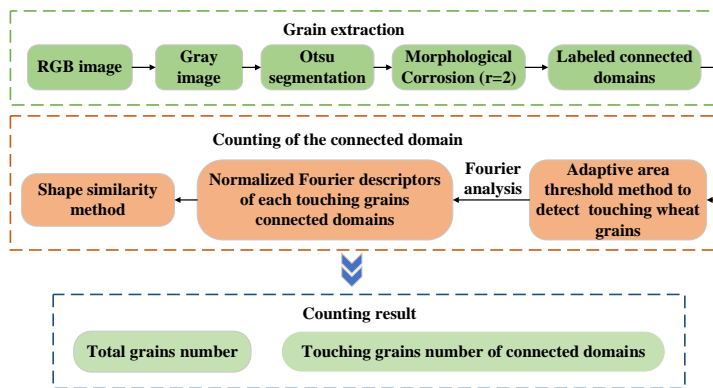


Fig. 2. Workflow diagram of the automatic counting method.

2.3.1. Grain extraction

The original image size was 3968×2976 pixels. The grain extraction process was described schematically in Fig. 3. Firstly, the RGB image was transformed to grayscale image, and the binary image was obtained by Otsu segmentation. Then morphological open operation was applied to remove small, isolated areas of noise. Finally, the connected regions were marked for subsequent counting of total grains number.

Otsu segmentation can select the optimal threshold by the maximum inter-class variance [27, 28]. Suppose there are L grey levels in the image. The probability distribution of each grey level can be calculated using Eq. (1) [27].

$$P_j = \frac{h_j}{H} \quad (1)$$

where H is the total number of pixels in the image, h_j is the number of pixels at level j [27].

$$H = \sum_{j=0}^{L-1} h_j \quad (2)$$

Let the pixels be dichotomized into parts C_0 and C_1 by a threshold t . C_0 and C_1 represent pixels resultant to the background and foreground, respectively. The class mean levels are given by Eq. (3) [28]. The total mean level of the image can be obtained from Eqs. (5) and (6) can be derived from the variance calculation formula [28]. Based on the basic principle of Otsu segmentation, the threshold that maximizes the δ^2 of C_0 and C_1 is the optimal threshold value of image.

$$\omega_0 = \frac{\sum_{j=0}^t P_j j}{P_0}, \omega_1 = \frac{\sum_{j=t+1}^l P_j j}{P_1} \quad (3)$$

$$\text{where } P_0 = \sum_{j=0}^t P_j, P_1 = \sum_{j=t+1}^l P_j \quad (4)$$

$$\omega_T = P_0 \omega_0 + P_1 \omega_1 \quad (5)$$

$$\delta^2 = P_0 (\omega_0 - \omega_T)^2 + P_1 (\omega_1 - \omega_T)^2 \quad (6)$$

Due to the influence of environment, there will be small, isolated areas of noise in the binary image. Morphological operations can be used to remove image noise and eliminate object boundary points by convolving the original image with structural elements [29]. The basic operations include corrosion and expansion. Corrosion and expansion can narrow and expand the target range respectively, which can be given by Eq. (7) [29]

$$A \ominus B = \{z | (B)_z \cap A^c = \Phi\}, A \oplus B = \{z | [(B)_z \cap A] \subseteq A\} \quad (7)$$

where A is the original image, B is a structural element, A^c is the complement set of A , Φ is an empty set.

Morphological open operation was applied to this paper, which uses corrosion first followed by expansion [29]. Small, isolated areas of noise can be eliminated when the size of structural element denoted by r is set to 2. Also, the connected regions were marked for subsequent counting.

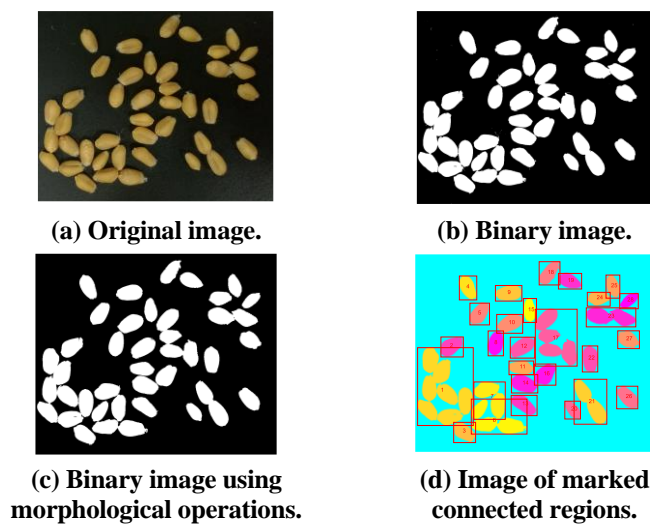


Fig. 3. The process of grain extraction.

2.3.2. The counting for the connected region formed by touching wheat grains

The problem of under-segmentation due to touching grains still needed to be addressed. The connected region formed by touching grains was detected using the adaptive area threshold method in an image, which was based on the median area of the connected region. The area of the connected region was considered as a

single kernel while was smaller than the area threshold. Otherwise, it was thought of as the touching grains. After that, Fourier analysis for the connected region was performed, which was shown in Fig. 4. Fourier analysis was used to obtain the shape of the connected region formed by touching grains. Then, the normalized Fourier descriptors $e(n)$ was identified. Finally, the grain number of connected region was counted by shape similarity method.

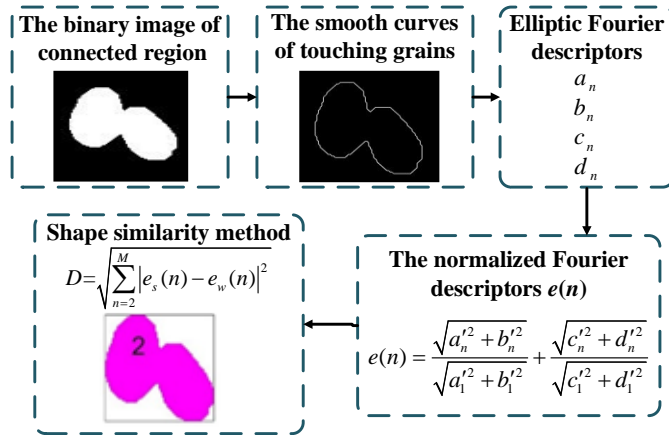


Fig. 4. Workflow diagram of the counting for the connected region formed by touching wheat grains using Fourier analysis.

The process of the elliptic Fourier series approximation represents a parametric solution. It was the presentation of the connected region boundary points (x, y) points as a pair of equations based on a third variable (i) . With the help of the 8-harmonic Fourier series, the discrete pixel contour information was converted into smooth curves as Fig. 5(a). The smooth curves on the x -axes $x(i)$ and the smooth curves on the y -axes $y(i)$ were shown in Fig. 5(b) and 5(c), respectively. Individual connected region boundary pixels were used to describe the chain code. They started with a given reference point and traced the boundary clockwise. When the reference point was reached, chain coding was completed. The elliptic Fourier series approximation of connected region projected on the x and y -axes can be given by Eq. (8) [21]. The elliptic Fourier descriptors of the n th harmonic (a_n, b_n, c_n, d_n) were calculated based on a discrete Fourier series approximation of chain-coded boundary contours, Eq. (9) [21].

$$\begin{aligned} x_j(i) &= a_0 + \sum_{n=1}^k a_n \cos\left(\frac{2n\pi i}{T}\right) + b_n \sin\left(\frac{2n\pi i}{T}\right) \\ y_j(i) &= c_0 + \sum_{n=1}^k c_n \cos\left(\frac{2n\pi i}{T}\right) + d_n \sin\left(\frac{2n\pi i}{T}\right) \end{aligned} \quad (8)$$

where i is the step required to move a unit pixel along the closed contour, T represents the total number of bounding points of connected regions, and k is the number of Fourier harmonics.

$$a_n = \frac{T}{2n^2\pi^2} \sum_{i=0}^{k-1} \frac{\Delta x_i}{\Delta i_i} \left(\cos\left(\frac{2n\pi i_i}{T}\right) - \cos\left(\frac{2n\pi i_{i-1}}{T}\right) \right)$$

$$\begin{aligned}
 b_n &= \frac{T}{2n^2\pi^2} \sum_{i=0}^{k-1} \frac{\Delta x_i}{\Delta i_i} \left(\sin\left(\frac{2n\pi i_i}{T}\right) - \sin\left(\frac{2n\pi i_{i-1}}{T}\right) \right) \\
 c_n &= \frac{T}{2n^2\pi^2} \sum_{i=0}^{k-1} \frac{\Delta y_i}{\Delta i_i} \left(\cos\left(\frac{2n\pi i_i}{T}\right) - \cos\left(\frac{2n\pi i_{i-1}}{T}\right) \right) \\
 d_n &= \frac{T}{2n^2\pi^2} \sum_{i=0}^{k-1} \frac{\Delta y_i}{\Delta i_i} \left(\sin\left(\frac{2n\pi i_i}{T}\right) - \sin\left(\frac{2n\pi i_{i-1}}{T}\right) \right)
 \end{aligned} \tag{9}$$

where Δi_i is the distances along the x and y axes between $(i-1)$ th and i th point, Δx_i is the distance along the x axes, Δy_i is the distance along the y axes.

$$\begin{aligned}
 \Delta x_i &= x_i - x_{i-1} \\
 \Delta y_i &= y_i - y_{i-1} \\
 \Delta i_i &= \sqrt{\Delta x_i^2 + \Delta y_i^2} \\
 T &= \sum_{i=1}^k \Delta i_i
 \end{aligned} \tag{10}$$

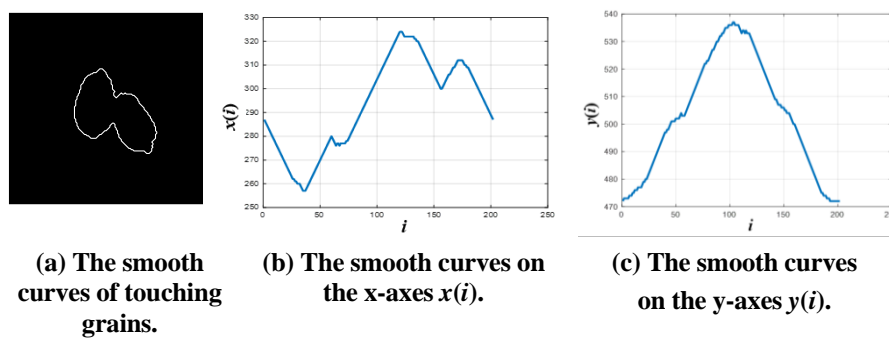


Fig. 5. Boundary detection and Fourier series approximation.

The Fourier coefficients obtained by the Fourier series of 8 harmonics vary with size, rotation, and the chain starting point of a contour. In consequence, they cannot be used as measures of variability in counting the number of touching grains. Fourier descriptors were further normalized by Eq. (11) [21, 30]. The normalized Fourier descriptors $e(n)$ was used to characterize connected regions formed by different number of wheat grain. Some cases of touching in the binary images were shown in Table 1, where $e(n)$ were the results of feature extraction by normalized Fourier descriptors of the Fourier series of 8 harmonics in different cases.














$$e(n) = \frac{\sqrt{a_n'^2 + b_n'^2}}{\sqrt{a_1'^2 + b_1'^2}} + \frac{\sqrt{c_n'^2 + d_n'^2}}{\sqrt{c_1'^2 + d_1'^2}} \tag{11}$$

where a'_n, b'_n, c'_n, d'_n are the standardized coefficients of the n th harmonic, a'_1, b'_1, c'_1, d'_1 are the standardized coefficients of the 1st harmonic, then [21]

$$\begin{bmatrix} a'_n & b'_n \\ c'_n & d'_n \end{bmatrix} = \frac{1}{E^n} \begin{bmatrix} \cos \varphi & \sin \varphi \\ \sin \varphi & \cos \varphi \end{bmatrix} \begin{bmatrix} a_n & b_n \\ c_n & d_n \end{bmatrix} \begin{bmatrix} \cos n \theta & -\sin n \theta \\ \sin n \theta & \cos n \theta \end{bmatrix} \tag{12}$$

$$\begin{cases} E = (a^{*2} + c^{*2})^{\frac{1}{2}} \\ \varphi = \arctan(c^*/a^*) \\ a^* = a_1 \cos \theta + b_1 \sin \theta \\ c^* = c_1 \cos \theta + d_1 \sin \theta \\ \theta = \frac{1}{2} \arctan(2(a_1 b_1 + c_1 d_1)/(a_1^2 + c_1^2 - b_1^2 - d_1^2)) \end{cases} \quad (13)$$

Table 1. $e(n)$ of different touching shapes.

Shape	$e(n)$							
	2.0000	0.4553	0.6966	0.1506	0.3657	0.0233	0.0472	0.0476
	2.0000	1.6837	2.0174	0.3557	1.0927	0.1934	0.2824	0.0764
	2.0000	1.3467	2.2381	0.5800	0.1540	0.4485	0.3067	0.5186
	2.0000	1.6127	1.7068	0.1574	0.2575	0.1114	0.2665	0.0593
	2.0000	1.0247	1.9008	0.1576	0.4753	0.2534	0.3817	0.0486
	2.0000	0.4460	0.4979	0.0481	0.0725	0.0112	0.0041	0.0195
	2.0000	0.4132	0.0907	0.1242	0.5203	0.0299	0.0400	0.0258
	2.0000	0.1290	0.9898	1.1751	0.6237	0.3676	0.0131	0.4983
	2.0000	3.9301	1.4388	1.2489	1.9337	0.5289	0.1613	0.5707
	2.0000	0.4195	0.2424	0.3454	0.2874	0.0986	0.1874	0.1093
	2.0000	0.3970	0.3039	0.1682	0.1322	0.5944	0.0589	0.0980
	2.0000	1.9184	0.8055	0.0171	0.4925	0.4344	0.1107	0.0991
	2.0000	0.2280	0.2453	0.0411	0.0238	0.0104	0.0209	0.0054

According to the standardized coefficients $e(n)$ had nothing to do with the chain starting point, rotation, and size of a connected region, the relationship between the grain number of the connected region and the normalized Fourier descriptors was identified. The datasets of different touching conditions were established in advance. The shape similarity method D uses Euclidean distance shown in Eq. (14), where s, w was the benchmark connected region in the datasets and test connected region, respectively [31]. And the grain number of connected region n_j was determined by shape similarity method. The shape similarity measure results between 13 cases of touching were shown in Table 2. It was shown that when the $D_{s,w}$ was less than 1.0000, the grain number of connected regions s, w were the same. The closer the value is to 0, the more the shape of the connected region w is similar to the connected region s . The under-segmentation regions were classified into 10, including two grains, three grains, ..., ten grains, or more than ten grains.

$$D = \sqrt{\sum_{n=2}^M |e_s(n) - e_w(n)|^2} \quad (14)$$

where $e_s(n)$ was the normalized Fourier descriptors of the benchmark connected region, $e_w(n)$ was the normalized Fourier descriptors of the test connected region.

Table 2. $D_{s,w}$ of different categories of adhesion.

	1	2	3	4	5	6	7	8	9	10	11	12	13
1	0.00 00	1.97 72	1.96 73	1.55 82	1.39 69	0.37 26	0.62 77	1.62 21	5.08 25	4.1 108	13.9 017	2.13 10	1.13 17
2	1.97 72	0.00 00	1.16 40	0.91 96	0.93 94	2.25 62	2.40 74	2.37 60	4.03 21	2.7 201	12.2 314	3.12 42	2.53 31
3	1.96 73	1.16 40	0.00 00	0.93 20	0.87 39	2.15 90	2.51 28	2.17 00	4.46 74	2.7 910	12.3 343	3.01 21	2.49 39
4	1.55 82	0.91 96	0.93 20	0.00 00	0.68 15	1.71 74	2.04 45	2.28 21	4.34 62	2.6 533	12.4 147	2.78 21	2.14 79
5	1.39 69	0.93 94	0.87 39	0.68 15	0.00 00	1.63 70	1.95 47	2.01 02	4.62 27	3.1 565	12.8 256	2.69 91	2.06 22
6	0.37 26	2.25 62	2.15 90	1.71 74	1.63 70	0.00 00	0.61 23	1.80 91	5.24 66	4.2 075	14.0 176	2.09 94	1.11 80
7	0.62 77	2.40 74	2.51 28	2.04 45	1.95 47	0.61 23	0.00 00	1.82 81	5.19 70	4.4 545	14.2 218	2.12 66	1.07 69
8	1.62 21	2.37 60	2.17 00	2.28 21	2.01 02	1.80 91	1.82 81	0.00 00	4.51 94	4.5 323	14.0 211	1.73 53	1.30 32
9	5.08 25	4.03 21	4.46 74	4.34 62	4.62 27	5.24 66	5.19 70	4.51 94	0.00 00	3.9 354	11.0 341	4.40 70	4.65 63
10	4.11 08	2.72 01	2.79 10	2.65 33	3.15 65	4.20 75	4.45 45	4.53 23	3.93 54	0.0 000	9.82 00	4.76 35	4.43 55
11	13.9 017	12.2 314	12.3 343	12.4 147	12.8 256	14.0 176	14.2 218	14.0 211	11.0 341	9.8 200	0.00 00	14.2 219	14.1 294
12	2.13 10	3.12 42	3.01 21	2.78 21	2.69 91	2.09 94	2.12 66	1.73 53	4.40 70	4.7 635	14.2 219	0.00 00	1.14 99
13	1.13 17	2.53 31	2.49 39	2.14 79	2.06 22	1.11 80	1.07 69	1.30 32	4.65 63	4.4 355	14.1 294	1.14 99	0.00 00

2.3.3. Counting of wheat grain number

Therefore, the number of grains in an image was represented by M :

$$M = m - N + \sum_{j=1}^n n_j \quad (15)$$

where N is the number of the connected region formed by touching grains, m is the total number of connected regions in the binary image, and n_j is the grain number of connected region j .

3. Results and Analysis

The designed counting method for touching wheat grains identified the relationship between the grain number of the connected region and the normalized Fourier descriptors by shape similarity method, which reduced grain counting errors led by improper grain separation and the computational complexity. The grain number of connected regions formed by touching grains was counting by the proposed methods and shown in Fig. 6. The standardized Fourier coefficients for each region were the input as shown in Table 3. The connected region (b1~b5) formed by touching grains was counted one-by-one. The number of counting results was shown in Table 3.

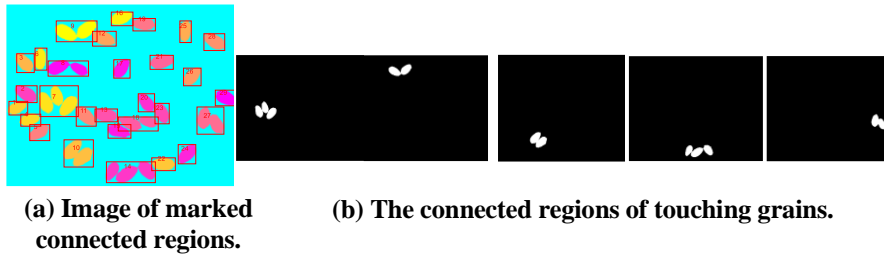


Fig. 6. Progress of the proposed method.

Table 3. $e(n)$ and counting results of the connected regions formed by touching grains.

		$e(n)$							Counting results
b1	2	0.1145	0.9595	1.0944	0.6076	0.3287	0.0322	0.4234	3
b2	2	1.8117	1.7004	0.1895	0.2768	0.1528	0.2549	0.0555	2
b3	2	0.6772	0.5439	0.2066	0.5581	0.0877	0.0416	0.0204	2
b4	2	0.8977	1.7072	0.6930	0.9919	0.1513	0.1204	0.0979	3
b5	2	0.5209	0.6636	0.1881	0.3899	0.0290	0.0776	0.0480	2

To demonstrate the counting accuracy, the existing algorithms were also used as comparisons in the paper. As indicated in Fig. 7, over-separation was caused by the watershed algorithm. The morphological corrosion method can availablely separate grains which are adhered slightly. But it often unable to produce an accurate separation. There is still a lot of potential for optimization of grain counting. And the proposed method was tested on wheat grains under different touching scenarios and compared with current counting methods with regard to error ratio and running time. The results were reported in Table 4. Equation (16) was a calculation of error ratio.

$$\text{Error ratio} = \frac{|M - M_0|}{M_0} \times 100\% \quad (16)$$

where M is the number of wheat grains calculated by the proposed method and existing main methods of grain counting, M_0 is the number of wheat grains counted manually.

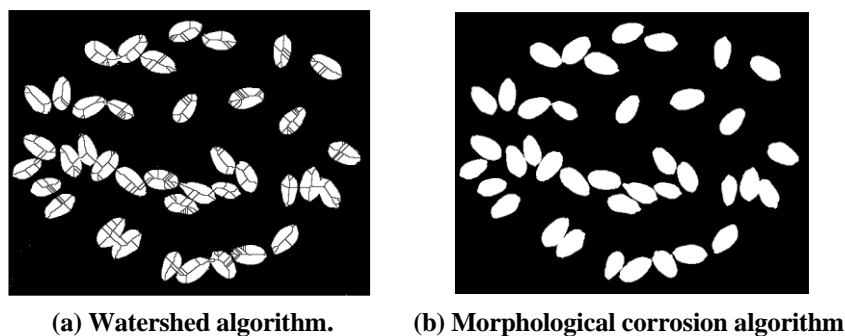


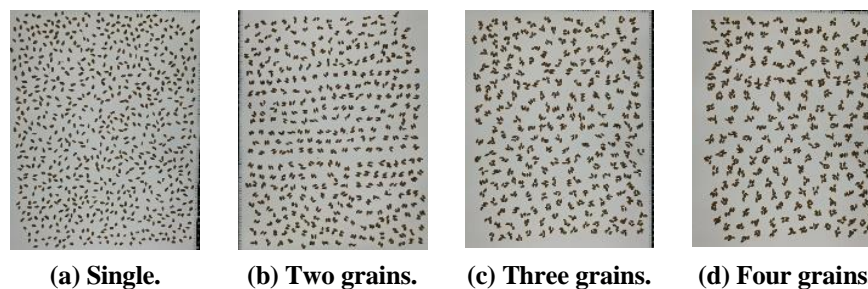
Fig. 7. Segmentation results using the watershed algorithm and the morphological corrosion algorithm.

Table 4. Counting result of different methods.

Manual counting number	Error ratio			
	Morphology erosion	Area estimation	Corner matching algorithm	Proposed method
20	0.25	0.4	0	0
32	0	0	0	0
38	0.1579	0	0.0175	0
38	0.0263	0	0.0187	0
49	0.1633	0.102	0.0234	0
54	0.2037	0.1481	0.0259	0.0185
74	0.1216	0.0946	0.0425	0.0241
80	0.3250	0.1075	0.0572	0.0275
Average accuracy	0.8440	0.8935	0.9769	0.9912
Average time/s	0.870	1.151	4.372	1.662

As shown in Table 4, it was apparent that the error ratios of the morphology erosion algorithm and the area estimation algorithm were more than that of the proposed algorithm and the corner matching algorithm. The more the number of wheat grains, the more the error ratio of the morphology erosion algorithm growing and the fewer the error ratio of the area estimation algorithm growing. The reason was that the complication of touching scenarios increased with the increase of grain number. And the increase in the amount of data lead to a decrease in the error rate of the area estimation method. The error ratio of the proposed method was below 3% and the average accuracy was 99.12%, which was significantly higher than those accuracy achieved by the morphology erosion algorithm and the area estimation algorithm, respectively. The average running time of the proposed method was 1.662s. In contrast to the corner algorithm, the run time is reduced while maintaining accuracy.

However, the error ratio of the proposed method was also relevant to the grain number per connected region. Further experiments of different fixed grain numbers per connected region were carried out to investigate this problem. The different fixed grain numbers per connected region (Fig. 8) were counted by the proposed method, morphology erosion, area estimation and corner algorithm. The results were shown in Figs. 9 and 10, where the x -axis represents the number of grains in different touching cases, and the y -axis represents the time and error rate for different methods, respectively. The counting results obtained with the proposed method for different numbers of connected regions were shown in Fig. 11.

**Fig. 8. The grain extraction process.**

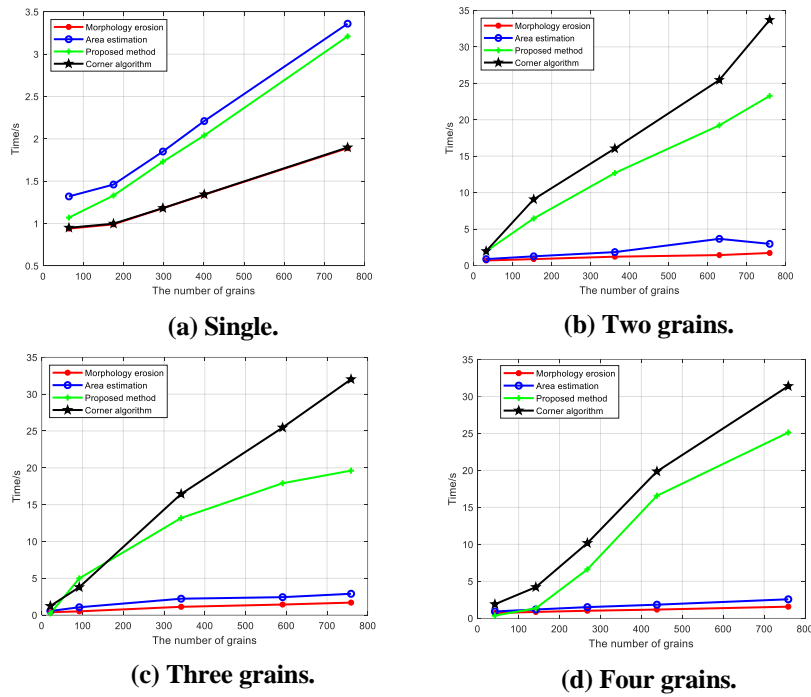


Fig. 9. Comparison of running times of different methods in different cases.

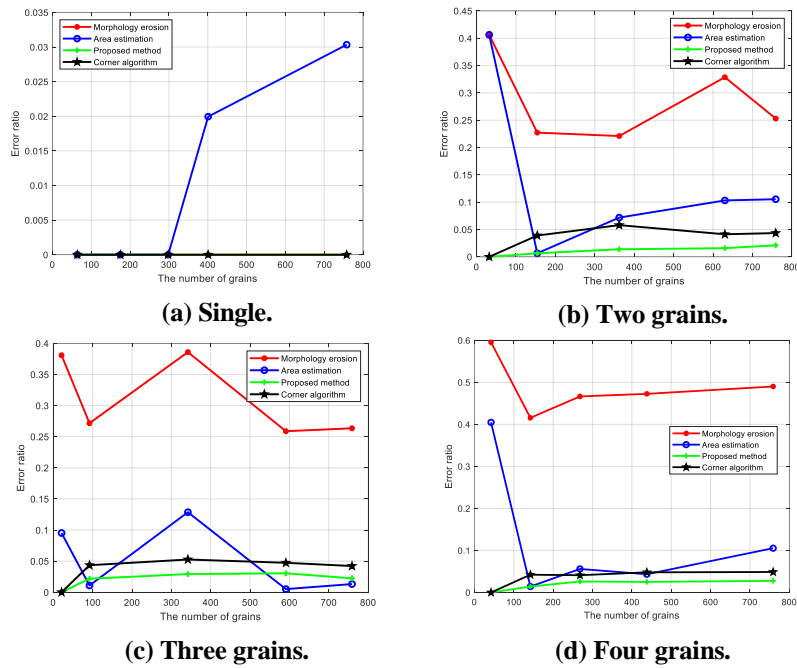


Fig. 10. Comparison of error ratio of different methods in different touching cases.

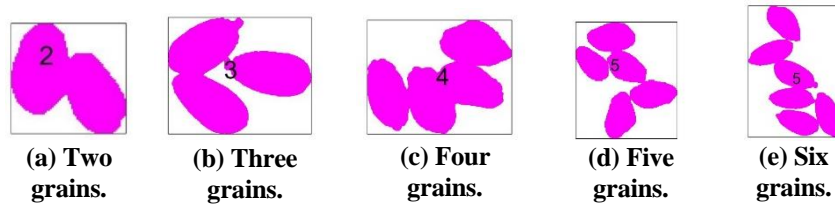


Fig. 11. The counting results for different touching cases.

As shown in Fig. 9, compared with the counting results using the corner matching algorithm, the computing time of the proposed method was less. The running time of area estimation and morphological erosion algorithms decreased with the increase of grain number. But the running time and the matching amount of the corner of the proposed method increased more. The increase in the number of the connected region formed by touching grains had little effect on the computing time of the proposed method. The more complex the shape of the connected region, the higher the error ratio of the proposed method.

As shown in Fig. 10, there was instability in the error rate of area estimation as the grain number per connected region increases. When the number of connected region was more than 150, the area estimation method had a higher accuracy. But the area threshold depended on human experience which was the most important factor affecting the counting accuracy of a few grains of wheat. The more complex the shape of the connected region, the higher the error rate of the proposed method, the corner matching algorithm and the morphology erosion. The error rate of morphological erosion increased more, but there was no substantial change in the proposed method and corner matching algorithm. The error ratio of the proposed method was also less than the error ratio of the corner matching algorithm. As shown in Fig. 11, due to the complexity of the connected area, counting errors may occur as the grain number of per connected region increases such as Fig. 11(e). However, when the grain number was 759, the error rate was still less than 3%. The grain number can be effectively counted was bigger than the number reported in the literature [4].

Although the proposed approach's running time grew with the number of grains, it was often no more than 25 seconds. The counting results of the same number of connected regions were shown in Table 5. It was different in touching numbers per connected region. It was apparent that the running time was associated with the number of the connected region formed by touching grains but was irrelevant to the grain number per connected region. The main novelty of the proposed method was the significant improvement of the computation accuracy for counting the complex touching grains while reducing calculation time.

Table 5. Counting results of the different touching numbers per connected region.

Grain number per connected region (Number of connected regions)	4 (82)	6 (81)	7 (78)	8 (81)	10 (78)
Running time/s	16.83	15.85	14.06	16.65	14.94
Error ratio	0.0296	0.0345	0.0412	0.0456	0.0585

4. Conclusions

In this paper, a novel automatic counting method for touching grains was proposed by using the Fourier analysis and shape similarity method. The following conclusions have been summarized as follow:

- The normalized elliptic Fourier descriptors was used to capture the shape of touching grains. Then, the grain number of the connected region formed by touching grains was identified by shape similarity method.
- The main novelty was the significant improvement of the computation accuracy for counting the complex touching grains while reducing calculation time. Compared with morphology erosion, area estimation and corner algorithm, the proposed method can reduce the running time since it does not require segmenting the touching grains before counting. At the same time, it overcomes the problems like over separation, matching errors or low segmentation accuracy for complex touching areas.
- The proposed method was tested on wheat grains under different touching scenarios and compared with existing counting methods. The error ratio and the average running time of counting grain number per spike were 2.75% and 1.662 seconds, respectively.
- The experiment of the fixed touching number was conducted, in which the number of touching grains per connected region was fixed and same. When the grain number was 759, the error rate was still less than 3%. What's more, the average accuracy of which was 99.12% and higher than average accuracy reported in the literature. Experimental results showed that the running time was associated with the number of connected regions but was irrelevant to the grain number per connected region.

Consequently, the automatic counting method for touching wheat grain could lay a solid foundation for future estimation of wheat yield.

Acknowledgement

We gratefully thank the support provided by “NSFC (No. 31871543)”, “Natural Science Foundation of Shandong (No. ZR2020KF002)” and Shandong Provincial Key Research and Development Program (Major Science and Technology Innovation Project) (No.2021LZGC013, 2022LZGCQY002).

Nomenclatures

A	The original image
A^c	The complement set of A
a_1'	The elliptic Fourier descriptor of 1st harmonic
a_n	The elliptic Fourier descriptor of n th harmonic
a_n'	The standardized coefficients of the n th harmonic
B	A structural element
b_1'	The elliptic Fourier descriptor of 1st harmonic
b_n	The elliptic Fourier descriptor of n th harmonic
b_n'	The standardized coefficients of the n th harmonic
C_0	The pixels resultant to the background

C_1	The pixels resultant to the foreground
c_1'	The elliptic Fourier descriptor of 1st harmonic
c_n	The elliptic Fourier descriptor of n th harmonic
c_n'	The standardized coefficients of the n th harmonic
D	Euclidean distance
d_1'	The elliptic Fourier descriptor of 1st harmonic
d_n	The elliptic Fourier descriptor of n th harmonic
d_n'	The standardized coefficients of the n th harmonic
$e(n)$	Normalized Fourier descriptors
$e_s(n)$	The normalized Fourier descriptors of the benchmark connected region
$e_w(n)$	The normalized Fourier descriptors of the test connected region
H	The total number of pixels in the image
h_j	The number of pixels at level j
i	Step required to move a unit pixel along the closed contour
k	Number of Fourier harmonics
L	Total number of grey levels
m	Total number of connected regions in the binary image
M	Number of wheat grains calculated by the proposed method and existing main methods of grain counting
M_0	Number of wheat grains counted manually
n_j	Grain number of connected region j
N	Number of the connected region formed by touching grains
P_0	The probability distribution of level from 0 to $z-1$
P_1	The probability distribution of level from z to $L-1$
P_j	The probability distribution of level j
r	The size of structural element
s	Benchmark connected region in the datasets
T	Total number of connected region boundary points
t	The threshold for segmenting image into foreground and background
x_j	Elliptic Fourier series approximation of connected region projected on the x -axis
y_j	Elliptic Fourier series approximation of connected region projected on the y -axis
Greek Symbols	
Δi_i	Distances along the x and y axes between $(i-1)$ th and i th point
Δx_i	The distances along the x axes
Δy_i	The distances along the y axes
δ^2	Inter-class variance of foreground and background
Φ	An empty set
ω_0	The mean level of C_0
ω_1	The mean level of C_1
ω_T	The total mean level of the image
Abbreviations	
TKW	Thousand Kernel Weight

References

1. Nagy, é.; Lehoczki-Krsjak, S.; Lantos, C.; and Pauk, J. (2018). Phenotyping for testing drought tolerance on wheat varieties of different origins. *South African Journal of Botany*, 116, 216-221.
2. Fan, X.L.; Cui, F.; Ji, J.; Zhang, W.; Zhao, X.Q.; Liu, J.J.; Meng, D.Y.; Tong, Y.P.; Wang, T.; and Li, J.M. (2019). Dissection of pleiotropic QTL regions controlling wheat spike characteristics under different nitrogen treatments using traditional and conditional QTL mapping. *Frontiers in Plant Science*, 10, 187.
3. García, G.A.; Serrago, R.A.; Dreccer, M.F.; and Miralles, D.J. (2016). Post-anthesis warm nights reduce grain weight in field-grown wheat and barley. *Field Crops Research*, 195, 50-59.
4. Wu, W.H.; Zhou, L.; Chen, J.; Qiu, Z.J.; and He, Y. (2018). (2018). GainTKW: A measurement system of thousand kernel weight based on the Android platform. *Agronomy*, 8(9), 178.
5. Zhou, L.; Wu, W.; Liu, T.; and Sun, C.M. (2020). Research status and prospect of rice and wheat grain counting methods. *Modern Agricultural Science and Technology*, 12, 18-20+22.
6. Shatadal, P.; Jayas, D.S.; and Bulley, N.R. (1995). Digital image analysis for software separation and classification of touching grains: I. disconnect algorithm. *Transactions of the ASAE*, 38(2), 645-649.
7. Quan, L.Z.; and Jiang, E.C. (2011). Automatic segmentation method of touching corn kernels in digital image based on improved watershed algorithm. *Institute of Electrical and Electronics Engineers*. Shandong, China, 34-37.
8. Zhang, H.; Tang, Z.H.; Xie, Y.F.; Gao, X.L.; and Chen, Q. (2019). A watershed segmentation algorithm based on an optimal marker for bubble size measurement. *Measurement*, 138, 182-193.
9. Liu, T.; Chen, W.; Wang, Y.F.; Wu, W.; Sun, C.M.; Ding, J.F.; and Guo, W.S. (2017). Rice and wheat grain counting method and software development based on Android system. *Computers and Electronics in Agriculture*, 141, 302-309.
10. Mebatsion, H.K.; and Paliwal, J. (2011). A Fourier analysis based algorithm to separate touching kernels in digital images. *Biosystems Engineering*, 108(1), 66-74.
11. Lin, P.; Chen, Y.M.; He, Y.; and Hu, G.W. (2014). A novel matching algorithm for splitting touching rice kernels based on contour curvature analysis. *Computers and Electronics in Agriculture*, 109, 124-133.
12. Tan, S.Y.; Ma, X.; Mai, Z.J.; Qi, L.; and Wang, Y.W. (2019). Segmentation and counting algorithm for touching hybrid rice grains. *Computers and Electronics in Agriculture*, 162(C), 493-504.
13. Wu, W.; Liu, T.; Zhou, P.; Yang, T.L.; Li, C.Y.; Zhong, X.C.; Sun, C.M.; Liu, S.P.; and Guo, W.S. (2019). Image analysis-based recognition and quantification of grain number per panicle in rice. *Plant Methods*, 15(1), 122.
14. Kaya, E.; and Saritas, İ. (2019). Towards a real-time sorting system: Identification of vitreous durum wheat kernels using ANN based on their morphological, colour, wavelet and gaborlet features. *Computers and Electronics in Agriculture*, 166, 105016.
15. Pun, C.M.; and An, N.Y. (2011). Image segmentation using effective region merging strategy. *International Journal of Digital Content Technology and its Applications*, 5(8), 59-69.

16. Bai, X.Z.; Sun, C.M.; and Zhou, F.G. (2009). Splitting touching cells based on concave points and ellipse fitting. *Pattern Recognition*, 42(11), 2434-2446.
17. Liu, Z.H.; Cheng, F.; and Zhang, W. (2016). A novel segmentation algorithm for clustered flexional agricultural products based on image analysis. *Computers and Electronics in Agriculture*, 126, 44-54.
18. Zhang, W.J.; and Li, H.Q. (2017). Automated segmentation of overlapped nuclei using concave point detection and segment grouping. *Pattern Recognition*, 71, 349-360.
19. Lin, P.; Chen, Y.M.; He, Y.; and Hu, G.W. (2014). A novel matching algorithm for splitting touching rice kernels based on contour curvature analysis. *Computers and Electronics in Agriculture*, 109, 124-133.
20. Yao, Y.; Wu, W.; Yang, T.L.; Liu, T.; Chen, W.; Chen, C.; Li, R.; Zhou, T.; Sun C.M.; and Zhou, Y. (2017). Head rice rate measurement based on concave point matching. *Scientific Reports*, 7(1), 41353.
21. Mebatsion, H.K.; Paliwal, J.; and Jayas, D.S. (2012). Evaluation of variations in the shape of grain types using principal components analysis of the elliptic Fourier descriptors. *Computers and Electronics in Agriculture*, 80, 63-70.
22. Delwiche, S.R.; Yang, I.C.; and Graybosch, R.A. (2013). Multiple view image analysis of freefalling U.S. wheat grains for damage assessment. *Computers and Electronics in Agriculture*, 98, 62-73.
23. Sokic, E.; and Konjicija, S. (2016). Phase preserving Fourier descriptor for shape-based image retrieval. *Signal Processing Image Communication*, 40(C), 82-96.
24. Tuset, V.M.; Galimany, E.; Farrés, A.; Marco-Herrero, E.; Otero-Ferrer, J.L.; Lombarte, A.; and Ramón, M. (2020). Recognising mollusc shell contours with enlarged spines: Wavelet vs Elliptic Fourier analyses. *Zoology*, 140, 125778.
25. Kupe, M.; Sayıncı, B.; Demir, S.; Ercişli, M.; and Baroň, J.S. (2021). Morphological characteristics of grapevine cultivars and closed contour analysis with Elliptic Fourier descriptors. *Plants*, 10(7), 1350.
26. Yang, C.Z.; and Yu, Q. (2018). Multiscale Fourier descriptor based on triangular features for shape retrieval. *Signal Processing: Image Communication*, 71, 110-119.
27. Bhandari, A.K.; Ghosh, A.; and Kumar, I.V. (2020). A local contrast fusion based 3D Otsu algorithm for multilevel image segmentation. *IEEE / CAA Journal of Automatica Sinica*, 7(1), 200-213.
28. Xue, F.; and Liu, L.Q. (2020). Image segmentation method of apple fruit spots based on Otsu algorithm. *Computer Technology and Development*, 30(12), 181-186.
29. Yan, H.W.; and Cui, Q.L. (2020). Hole filling in oat grain recognition based on morphological opening. *Agricultural Technology & Equipment*, 364(4), 10-11.
30. Chen, B.; Rao, H.H.; and Liu, M.H. (2020). Oleander fruit identification based on Fourier descriptors and Hu-invariant moments. *Journal of Zhejiang Agricultural Sciences*, 61(9), 1876-1880.
31. Zou, Y.; Chen, W.J.; Tong, M.Y.; and Tao, S. (2021). DEA cross-efficiency aggregation with deviation degree based on standardized Euclidean distance. *Mathematical Problems in Engineering*, 2021, 1-10.